Fast magic angle spinning for the characterization of milligram quantities of organic and biological solids at natural isotopic abundance by 13C–13C correlation DNP-enhanced NMR

Adam Smith, Rania Harrabi, Thomas Halbritter, Daniel Lee, Fabien Aussenac, Patrick C.A. van der Wel, Sabine Hediger, Snorri Th. Sigurdsson, Gaël de Paëpe

Fast Magic Angle Spinning for the Characterization of Milligram Quantities of Organic and Biological Solids at Natural Isotopic Abundance by ^{13}C-^{13}C correlation DNP-enhanced NMR

Adam N. Smith,[a⊥] *Rania Harrabi,*[a⊥] *Thomas Halbritter,*[b] *Daniel Lee,*[a] *Fabien Aussenac,*[c] *Patrick C. A. van der Wel,*[d] *Sabine Hediger,*[a] *Snorri Th. Sigurdsson,*[b] *and Gaël De Paëpe**[a].

[a] Univ. Grenoble Alpes, CEA, CNRS, IRIG, MEM, 38000 Grenoble, France

[b] University of Iceland, Department of Chemistry, Science Institute, Dunhaga 3, 107 Reykjavik, Iceland

[c] Bruker BioSpin, Wissembourg, France

[d] Zernike Institute for Advanced Materials, University of Groningen, Nijenborgh 4, 9747 AG Groningen, Netherlands.

[⊥] These authors contributed equally.

Corresponding Author

* gael.depaepe@cea.fr

HIGHLIGHTS

- Unprecedented sensitivity using recently developed AsymPol-POK hyperpolarizing agent
- Carbon-carbon correlation experiments at natural abundance on 1-2 mg of sample
- Examples on amyloid fibrils and microcrystals of pharmaceuticals at natural isotopic abundance

ABSTRACT

We show that multidimensional solid-state NMR ^{13}C-^{13}C correlation spectra of biomolecular assemblies and microcrystalline organic molecules can be acquired at natural isotopic abundance with only milligram quantities of sample. These experiments combine fast Magic Angle Spinning of the sample, low-power dipolar recoupling, and dynamic nuclear polarization performed with AsymPol biradicals, a recently introduced family of polarizing agents. Such experiments are essential for structural characterization as they provide short- and long-range distance information. This approach is demonstrated on diverse sample types, including polyglutamine fibrils implicated in Huntington's disease and microcrystalline ampicillin, a small antibiotic molecule.

GRAPHICAL ABSTRACT

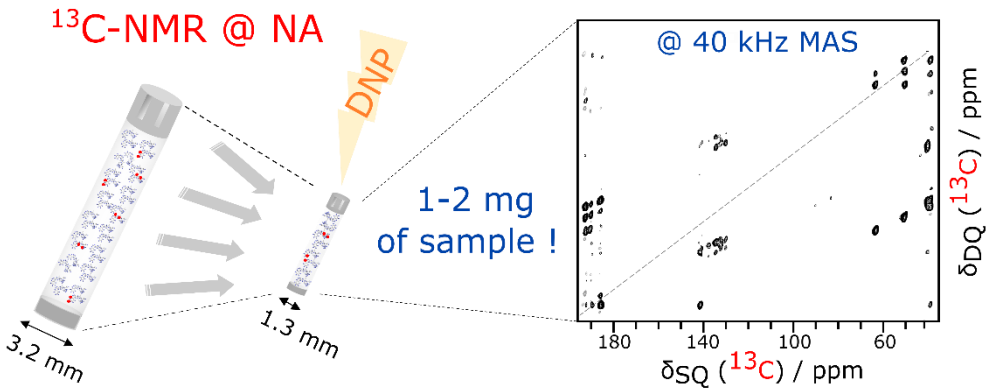

KEYWORDS. Dynamic Nuclear Polarization, MAS-DNP, Nuclear Magnetic Resonance, Fast MAS, Pharmaceuticals.

1. INTRODUCTION

Structural and dynamical characterization of solids at the atomic scale remains a salient, but difficult task. Magic Angle Spinning solid-state NMR (MAS ssNMR) has proved to be particularly adept at characterizing amorphous to microcrystalline solids ranging from biomolecules to materials [1,2]. Two major axes of methodological development have focused on fast MAS *(i.e.* sample rotation frequencies > 25 kHz) [3,4] and sensitivity enhancement through dynamic nuclear polarization (DNP) [5–11]. With the recent development of both cryogenic fast MAS probes and DNP technologies, these two axes are now combined [12–16].

Faster MAS rates provide numerous experimental benefits, including more efficient averaging of anisotropic interactions (which is particularly important for high magnetic fields), longer coherence lifetimes, and larger and more homogenous radiofrequency field strengths *(i.e.* B_1) as a result of the smaller coil dimension [4]. To achieve these fast MAS rates, a smaller sample rotor diameter (*i.e.* outer diameter < 3.2 mm) is required, which restricts sample volumes (*e.g.* ~ 2.5 µL in a Bruker 1.3 mm rotor *vs.* ~ 30 µL in a Bruker 3.2 mm rotor). Such a drastic reduction in sample volume can be advantageous when the sample amount is limited to a few milligrams or less, but also clearly impacts the overall signal-to-noise ratio. This is especially true for the detection of diluted spins with low gyromagnetic ratio (*e.g.* ^{13}C, ^{15}N). The loss in sensitivity due to the smaller sample volume can in part be mitigated by using indirect detection approaches, via ^{1}H spins [17,18]. In solids, this generally requires a MAS frequency > 40 kHz to substantially reduce the proton linewidths, thus increasing the signal-to-noise ratio, and then benefits from the excellent receptivity of proton spins [19–22]. As a consequence, ^{1}H-detected fast MAS 2D X-^{1}H heteronuclear correlation (HETCOR) experiments have been implemented in recent years for samples at natural isotopic abundance (NA), while correlation experiments under fast MAS

between less receptive nuclei (*e.g.* ^{13}C-^{13}C and ^{13}C-^{15}N) could only be applied to isotopically-enriched samples owing to the associated sensitivity limitations [23–28].

DNP is used to boost the sensitivity of ssNMR experiments by transferring the relatively larger polarization of unpaired electrons to NMR-active nuclei of interest. Currently, the most efficient high-field MAS-DNP mechanism is the cross-effect (CE), which often relies on the use of bisnitroxide paramagnetic dopants [29–36], although efficient heteroradicals have also been introduced [37–40]. The corresponding transfer of polarization is driven through periodic energy-level (anti-)crossings of the coupled spin system composed of the two electrons and the surrounding nuclei [41,42]. As the MAS rate increases, these energy level crossings may become less efficient, which decreases the DNP efficiency and lengthens the hyperpolarization build-up time [43–45]. This is notably the case for polarizing agents (PAs) with small to moderate electron-electron couplings (dipolar coupling and/or *J* exchange interaction). This is one of the reasons why we recently introduced the AsymPol family of polarizing agents, which was designed to have large effective electron-electron $|2J+D|$ couplings between the two nitroxide moieties in the biradical [35]. This leads to efficient transfers of polarization at the different energy level crossings, which results in short hyperpolarization build-up time constants (T_B) [35,46]. As such, this class of PAs is particularly adapted for DNP with fast MAS and herein we illustrate their use in this regime.

We show that fast MAS, combined with DNP and PAs particularly suited to this regime, can overcome previous sensitivity limitations and enables the acquisition of multidimensional correlation spectra of low abundant nuclei at NA (*e.g.* ^{13}C-^{13}C) on milligram-scale sample quantities. This is illustrated with polyglutamine (polyQ) amyloid fibrils (implicated in Huntington's disease) [47] and microcrystals of the antibiotic molecule ampicillin. Such experiments are typically orders of magnitude more demanding in terms of sensitivity than ^{1}H-X HETCOR-type experiments, but can provide extremely valuable information.

2. MATERIAL AND METHODS

All experiments were performed on a 9.4 T Bruker Avance III spectrometer equipped with a 263 GHz gyrotron and a corrugated waveguide to transfer the microwave irradiation to the Bruker 1.3 mm MAS DNP probe cooled to ~ 100 K. The probe was in double resonance $^{1}H/^{13}C$ configuration. The various DNP samples were impregnated with a DNP matrix containing 5 to 40 mM AsymPol-POK or cAsymPol-POK. The detailed preparation, matrix composition and radical concentration is given in the Supporting Information for each sample. The sample amount in the 1.3 mm rotor was ~1 mg for LecA and $D_2Q_{15}K_2$ fibrils and ~2 mg for ampicillin. The DNP experiments were run at a MAS frequency between 35 and 40 kHz. All 2D ^{13}C-^{13}C DQ/SQ dipolar correlation NMR experiments were acquired with the S_3 recoupling sequence [48,49].. The sequence and precise parameter settings for the different experiments are given in the Supporting Information.

3. RESULTS AND DISCUSSION

3.1. DNP-enhanced ^{13}C-^{13}C dipolar correlation experiments with fast MAS and low-power recoupling

Access to faster MAS alone has extra built-in benefits: *e.g.* it enhances the use of low-power ^{13}C-^{13}C dipolar recoupling sequences. Importantly, this allows the safe use of long mixing periods compatible with both long-distance polarization transfers and current radio-frequency (RF) hardware limitations, while keeping a relatively large ^{13}C excitation bandwidth. This is illustrated in Figure 1, which shows a ^{13}C-^{13}C double-quantum single-quantum (DQ-SQ) dipolar correlation experiment obtained on the uniformly labeled protein LecA (12.76 kDa). This experiment was recorded using the low-power dipolar recoupling sequence S_3, for which the recoupling condition requires the RF field strength to match half the MAS frequency [48], thus limiting the spectral bandwidth on which the recoupling is effective to about that value [49]. As illustrated in Figure 1,

access to the faster spinning of about 40 kHz enables the acquisition of a broadband DQ-SQ S_3 correlation spectrum encompassing all ^{13}C resonances for the protein, which is not possible at lower MAS rates. Indeed, at 13 kHz MAS, the S_3 sequence would only achieve a recoupling bandwidth of ~ 6.5 kHz [48,49], prohibiting observation of broadband correlations from carbonyl/aromatic to aliphatic carbons. The DNP enhancement for the experiment of Figure 1 was obtained using cAsymPol-POK as PA, as it was recently shown to be very efficient at polarizing proton-dense molecular systems [46]. Consistent with the characteristics of the AsymPol biradical family [35,46], a high DNP enhancement of 130 was obtained at 9.4 T and 39.8 kHz MAS, accompanied by a very short build-up time, T_B, of 0.5 s. The spectrum presented in Figure 1 was recorded in about 6 h with ~1 mg of protein sample. It can be noted that this experiment could also be collected in tens of minutes with a reasonable sensitivity. As is the case for ssNMR studies of proteins at room temperature, ^{13}C-^{13}C correlation spectra are one of the cornerstones of biomolecular DNP, particularly for the study of large systems or the observation of cryo-trapped intermediates. This approach can be combined with specific and sparse labeling, as well as targeted and selective DNP approaches to compensate for the limited resolution resulting from low temperature DNP-NMR measurements [50,51].

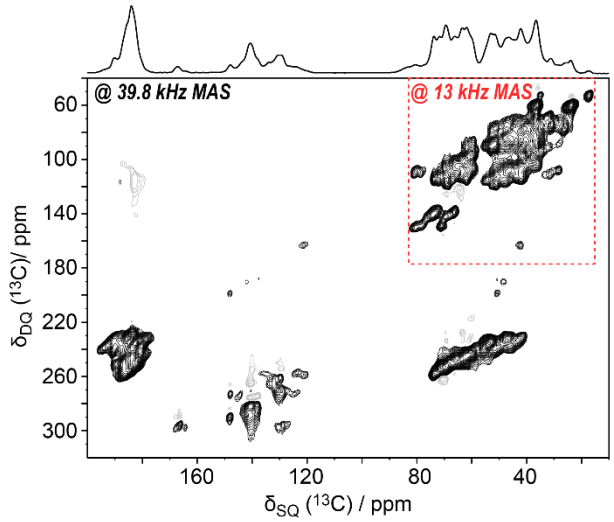

Figure 1. DNP-enhanced ^{13}C-^{13}C DQ-SQ dipolar correlation spectrum of ~ 1 mg of U-^{13}C, ^{15}N LecA, using the recoupling sequence S_3 [48,49] at 9.4 T and 39.8 kHz MAS. The sample was prepared by impregnating the protein pellet with 40 mM cAsymPol-POK glycerol-d_8/D_2O solution (60:40 v/v). The maximum recoupling bandwidth, which would have been achieved at 13 kHz MAS frequency, is highlighted with a red dashed square. See Supporting Information for more experimental details.

3.2. Application on natural isotopic abundance fibrils

Considering the excellent sensitivity of the fast MAS-DNP spectrum obtained with cAsymPol-POK on only one milligram of ^{13}C/^{15}N-labeled protonated biomolecule, we wondered if it was even necessary to isotopically enrich the sample? Recently, the first steps towards multidimensional ^{13}C-^{13}C and ^{13}C-^{15}N experiments at NA have been demonstrated on samples containing tens of milligrams. This was achieved at 9.4 T using MAS-DNP with a relatively large sample holder (*i.e.* 3.2 mm outer diameter) and spinning at MAS frequencies less than 15 kHz [30,46,52–65]. Through-bond (*i.e. J* based) [66] and through-space (*i.e.* dipolar coupling based) [67] experiments were reported and used, for instance, to determine the *de novo* assignment of a self-assembled 2'-deoxyguanosine derivative presenting two different molecules in the asymmetric crystallographic unit cell [61]. Beyond the fact that NA NMR is of interest for systems that cannot be easily isotopically labeled, additional benefits of working at NA were further illustrated. More specifically, it was demonstrated that the ^{13}C-^{13}C spin dynamics of small organic molecules at NA can be treated as a superposition of individual dipolar build-up contributions from intra- and inter-molecular spin pairs [62], which enables internuclear distances of up to ~ 7 Å to be probed [64]. This would not be possible for fully isotopically-enriched systems. Subsequently, the approach was applied to disease-relevant protein aggregates, for which spectral fingerprints as

well as dipolar build-ups were demonstrated [52], and extended to magnetic fields larger than 10 T [38].

Despite the utility of these studies, made with larger sample holders and lower spinning frequencies, there are numerous advantages to pursuing similar experiments under fast MAS with 1.3 mm (and smaller) rotors for the reasons mentioned above. In particular, it addresses the structural characterization of mass-limited samples that cannot be obtained in large amounts and/or for which isotopic enrichment is not feasible, as for example synthetic and natural small molecules. This is illustrated in Figure 2 on NA polyglutamine (polyQ) amyloid fibrils composed of the polyQ peptide $D_2Q_{15}K_2$, which features an analogous atomic structure to the aggregated state of disease-causing polyQ proteins. In this DQ-SQ ^{13}C-^{13}C dipolar correlation spectrum, acquired at 40 kHz MAS on only ~1 mg of fibrils, we choose a long mixing time (23 ms) to allow polarization transfer over long distances (up to about 7 Å [64]) within the polyQ amyloid core. At NA, ^{13}C–^{13}C spin pairs are only 0.01 % abundant, and as such long-range distance restraints can be probed without the interfering effects of dipolar truncation [54]. This type of correlation spectrum is ideal for differentiating between polymorphic structures [52]. For example, we clearly observe Cα–Cα and C′–C′ correlations from the polyQ backbone, which report on the β–strand configuration of the amyloid core, and Cα–C′/Cδ correlations, which report on side chain conformations [52]. Access to such long-distance constraints directly necessitates the ability to apply RF irradiation for long recoupling times. The use of low-power sequences like S_3 [48,49] while maintaining an efficient recoupling over the entire spectral bandwidth is essential in this case [64] and only possible with fast MAS.

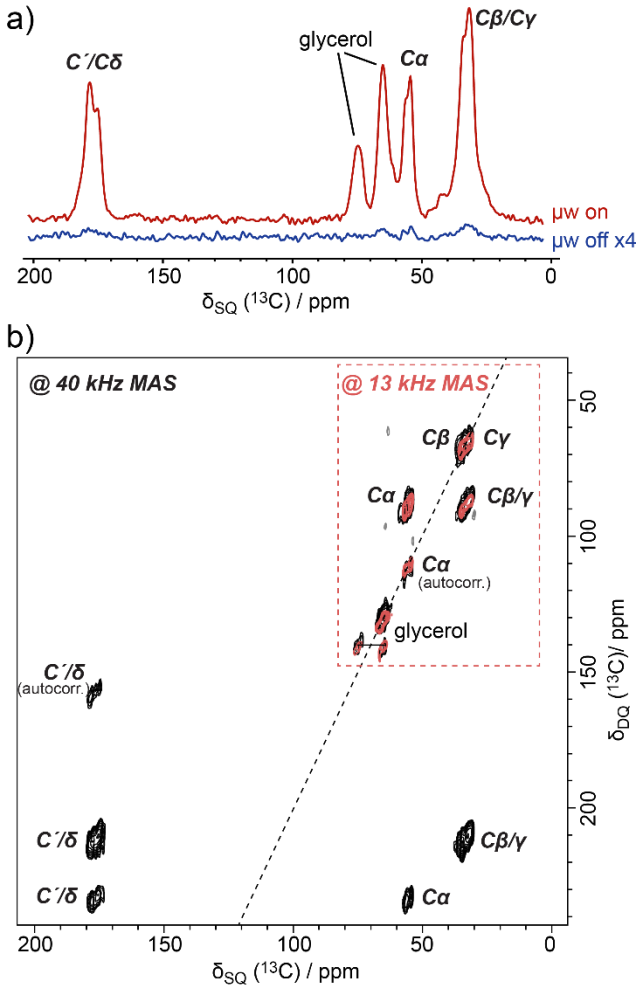

Figure 2. (a) ^{1}H-^{13}C CP spectra at a MAS frequency of 40 kHz on ~ 1 mg of polyQ amyloid fibrils formed by $D_2Q_{15}K_2$ with (red top trace) and without microwave (µw) (blue bottom trace) irradiation. The spectra were scaled to compensate for different numbers of co-added transients, to allow for intensity comparison. The sample was prepared with 5 mM AsymPol-POK glycerol-d_8/D_2O/H_2O solution (30:60:10 v/v/v). The DNP enhancement, measured by taking the ratio of signal intensity with and without µw irradiation, is 75. The DNP build-up time, T_B, was 3.1 s. (b) Superimposed DNP-enhanced ^{13}C-^{13}C DQ-SQ dipolar correlation spectra on the same sample as in (a), recorded using 13.55 kHz (red) and 40 kHz (black) MAS frequencies (3.2 and 1.3 mm probes, respectively). Assignment for the ^{13}C nuclei from the glutamine residues in the polyQ

amyloid core is given in the figure, based on our previous work [52]. Long-range inter-residue Cα and C'/δ autocorrelation peaks are clearly present. Note that the C'/ δ autocorrelation peak is folded in the indirect dimension. All the spectra were acquired at 9.4 T. See Supporting Information for more experimental details.

3.3. Application to natural isotopic abundance microcrystals

Efficient hyperpolarization of the fibrils benefits from the fact that one of the fibril dimensions is on the nanometer scale. The electron polarization, initially transferred from the PAs to the surface protons of the system, can easily be transferred across the width of the fibrils by proton-proton spin-diffusion, ensuring a homogeneous polarization of the nanofibrils [68]. In contrast, hyperpolarizing microcrystals of small organic molecules poses a greater challenge and requires the use of PAs that are particularly suited to polarize proton-dense systems, such as the ones of the AsymPol family [35,46]. The efficient transfer of polarization of these radicals is supported by relatively short build-up times, even under fast MAS conditions, which allows hyperpolarization to diffuse through the particles in a time shorter than the intrinsic nuclear relaxation time, T_{1n}. Thus, using AsymPol-POK and cAsymPol-POK, we were able to obtain DNP-enhanced ^{1}H-^{13}C heteronuclear (HETCOR) and ^{13}C-^{13}C DQ-SQ dipolar correlation experiments at 40 kHz MAS on only 2 mg of ampicillin at NA (see Figure 3). Although ^{1}H-^{13}C HETCOR experiments on organic microcrystalline solids can usually be recorded with standard ssNMR, DNP is needed for mass-limited synthetic small molecules and very useful to shorten experimental time, especially in the case of long ^{1}H T_1 relaxation times. Extending 2D ssNMR on NA samples also to ^{13}C-^{13}C correlation experiments is orders of magnitude more challenging in terms of sensitivity. From the spectra presented in Figure 3, we were able to find all expected ^{13}C resonances of the molecule

(assignment based on Ref. [69]), with the exception of the two methyl groups (carbons 9, 10) and carbons 2 and 5, which are not resolved in the 2D experiments.

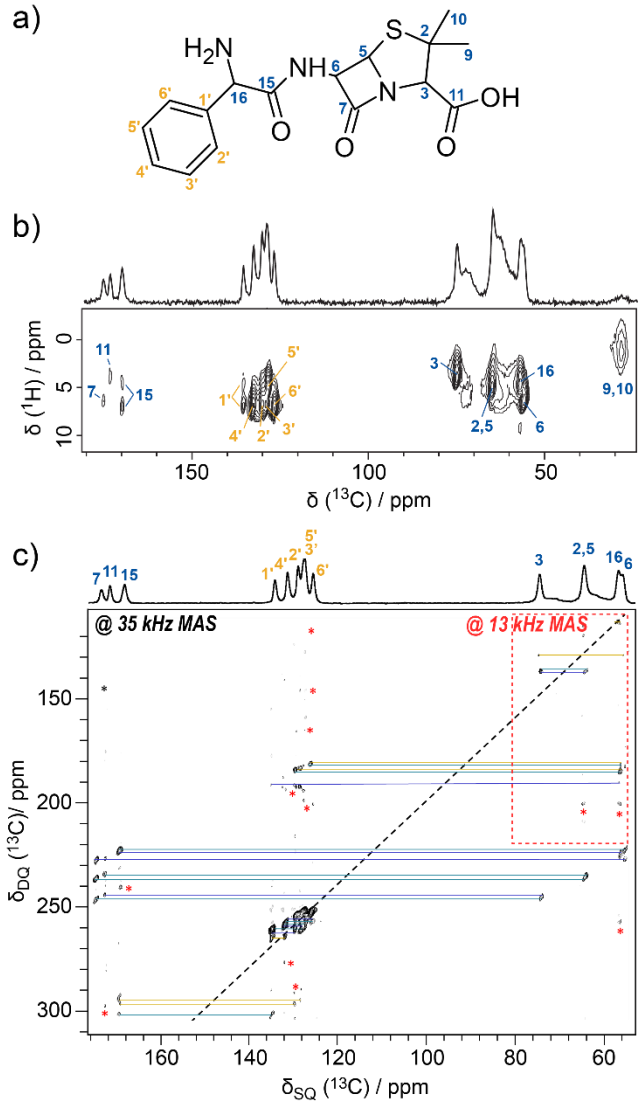

Figure 3. (a) Chemical structure of ampicillin. (b) DNP-enhanced 2D ^{1}H-^{13}C HETCOR dipolar correlation spectrum of ~2 mg of microcrystalline ampicillin at NA. A 200 µs CP contact time was used to ensure the observation of only short-range correlations. The MAS frequency was 40 kHz. The ampicillin powder was impregnated with 5 mM of AsymPol-POK in glycerol-d_8/D_2O/H_2O solution (30:60:10 v/v/v). The ^{13}C assignment given in the spectrum is based on the published assignment [69] (c) DNP-enhanced 2D ^{13}C-^{13}C DQ-SQ dipolar correlation spectrum using the

recoupling sequence S_3 [48,49] at 35 kHz MAS on a similar sample of ampicillin impregnated with 40 mM of cAsymPol-POK in glycerol-d_8/D_2O/H_2O solution (60:30:10 v/v/v). The ^{13}C assignment is mapped out in the 2D spectrum, which yields short-range (equivalent to one-bond and two-bond in blue and cyan, respectively) and long-range (three-bonds and more in yellow) correlations (based on the known assignment [69]). Signals from spinning sidebands, t_1-noise, and solvent are indicated with red asterisks. The interference of the methyl rotation frequency at 100 K with RF pulses led to a reduced sensitivity for the methyl resonances. (see projection on top of the spectrum in panel b), and as a result homonuclear correlations with the methyl carbons are not visible (region therefore not shown). The maximum recoupling bandwidth, which would have been achieved at 13 kHz MAS frequency, is highlighted with a red dashed square. All spectra were acquired at 9.4 T. See Supporting Information for more experimental details.

4. CONCLUSION

In conclusion, we have shown that ^{13}C multidimensional correlation spectra can be acquired with only milligram quantities of sample at NA. More specifically, broadband ^{13}C-^{13}C dipolar correlation spectra, only possible under fast MAS, were acquired on biomolecular aggregates and microcrystaline small molecules, both at NA. The newly developed PAs of the AsymPol family, such as AsymPol-POK and cAsymPol-POK [35,46], made these experiments feasible in a reasonable amount of time, thanks to their short hyperpolarization build-up times which increase the overall sensitivity of these DNP experiments under fast MAS.

In addition to the added spectroscopic benefits of performing experiments at fast MAS, the demonstrated feasibility of such experiments for small amounts of sample at NA also opens avenues for the characterization of sample types that were, so far, not amenable to ssNMR analysis. In particular, the characterization of *ex-vivo* amyloid fibrils from patient- or animal-derived

systems is an intriguing aspect of research associated with numerous neurodegenerative disorders [70,71]. As it is well known that amyloid fibrils adopt polymorphic structures and that the cellular milieu (*i.e.* molecular crowding, interaction with chaperones, post-translation modifications, etc.) can dictate the adopted conformation, it is imperative to study aggregates that are formed under native conditions [72]. With the method demonstrated here, one can now envision the study of *ex-vivo* amyloids at NA in the milligram quantities available from these systems.

The work presented here should also prove impactful for the study of natural products that are of great importance for numerous medicinal purposes. Indeed, a continued hurdle in the use and development of natural products, *e.g.* as new drug candidates, is their characterization, because they are typically isolated in small quantities. The structural information that can be gained from ssNMR is also invaluable for the characterization of other small molecules and their formulations. Finally, applications to other types of organic or hybrid (nano)materials, including thin films, can be enabled by these types of 2D NA ssNMR studies. The ability to rapidly characterize milligram quantities with multidimensional correlation experiments, as demonstrated here, will enable more routine use of ssNMR in these endeavors.

ASSOCIATED CONTENT

Supporting Information. Detailed sample preparation, experimental parameters for all MAS-DNP experiments. The PDF file is available free of charge.

AUTHOR INFORMATION

Notes

⊥ These authors contributed equally.

ACKNOWLEDGMENT

The authors thank O. Dakhlaoui for providing the labelled LecA sample, and I. Matlahov and R. Kodali for previously preparing the polyQ peptide sample. This work was funded by the European Union's Horizon 2020 research and innovation programme under the Marie-Skłodowska-Curie Action-795423-BOLD-NMR (to A.N.S.) and the European Research Council Grant ERC-CoG-2015 No. 682895 (to G.D.P.). In addition, this work was partially supported by funding from the French National Research Agency (CBH-EUR-GS and Labex ARCANE ANR-17-EURE-0003, Glyco@Alps ANR-15-IDEX-02, and ANR-16-CE11-0030-03), the Deutsche Forschungsgemeinschaft (DFG) through a postdoc fellowship (414196920), the University of Iceland Research Fund, and NIH grant R01 GM112678 (P.v.d.W.).

REFERENCES

[1] M. Renault, A. Cukkemane, M. Baldus. Solid-State NMR Spectroscopy on Complex Biomolecules, Angew. Chemie Int. Ed. 49 **(**2010**)** 8346–8357.

[2] D. L. Bryce. NMR crystallography: structure and properties of materials from solid-state nuclear magnetic resonance observables, IUCrJ 4 **(**2017**)** 350–359.

[3] A. Samoson, T. Tuherm, Z. Gan. High-Field High-Speed MAS Resolution Enhancement in ^{1}H NMR Spectroscopy of Solids, Solid State Nucl. Magn. Reson. 20 **(**2001**)** 130–136.

[4] Y. Nishiyama. Solid-State NMR Under Ultrafast MAS Rate of 40–120 kHz, in *Experimental Approaches of NMR Spectroscopy* **(Springer Singapore, 2018).** 171–195. doi:10.1007/978-981-10-5966-7_6

[5] V. S. Bajaj, C. T. Farrar, M. K. Hornstein, I. Mastovsky, J. Vieregg, J. Bryant, B. Eléna, K. E. Kreischer, R. J. Temkin, R. G. Griffin. Dynamic nuclear polarization at 9 T using a novel

250 GHz gyrotron microwave source, J. Magn. Reson. 160 (2003) 85–90.

[6] M. K. Hornstein, V. S. Bajaj, R. G. Griffin, R. J. Temkin. Continuous-wave operation of a 460-GHz second harmonic gyrotron oscillator, IEEE Trans. Plasma Sci. 34 (2006) 524–533.

[7] A. B. Barnes, G. De Paëpe, P. C. A. van der Wel, K.-N. Hu, C.-G. Joo, V. S. Bajaj, M. L. Mak-Jurkauskas, J. R. Sirigiri, J. Herzfeld, R. J. Temkin, R. G. Griffin. High-Field Dynamic Nuclear Polarization for Solid and Solution Biological NMR, Appl. Magn. Reson. 34 (2008) 237–263.

[8] A. B. Barnes, M. L. Mak-Jurkauskas, Y. Matsuki, V. S. Bajaj, P. C. A. van der Wel, R. Derocher, J. Bryant, J. R. Sirigiri, R. J. Temkin, J. Lugtenburg, J. Herzfeld, R. G. Griffin. Cryogenic sample exchange NMR probe for magic angle spinning dynamic nuclear polarization., J. Magn. Reson. 198 (2009) 261–70.

[9] A. J. Rossini, A. Zagdoun, M. Lelli, A. Lesage, C. Cop, L. Emsley, C. Copéret, L. Emsley. Dynamic Nuclear Polarization Surface Enhanced NMR Spectroscopy, Acc. Chem. Res. 46 (2013) 1942–1951.

[10] D. Lee, S. Hediger, G. De Paëpe. Is solid-state NMR enhanced by dynamic nuclear polarization?, Solid State Nucl. Magn. Reson. 66–67 (2015) 6–20.

[11] A. N. Smith, J. R. Long. Dynamic Nuclear Polarization as an Enabling Technology for Solid State Nuclear Magnetic Resonance Spectroscopy, *Analytical Chemistry* 88 (2016) 122–132.

[12] S. R. Chaudhari, P. Berruyer, D. Gajan, C. Reiter, F. Engelke, D. L. Silverio, C. Copéret, M. Lelli, A. Lesage, L. Emsley. Dynamic nuclear polarization at 40 kHz magic angle

spinning, Phys. Chem. Chem. Phys. 18 **(**2016**)** 10616–10622.

[13] S. R. Chaudhari, D. Wisser, A. C. Pinon, P. Berruyer, D. Gajan, P. Tordo, O. Ouari, C. Reiter, F. Engelke, C. Copéret, M. Lelli, A. Lesage, L. Emsley. Dynamic Nuclear Polarization Efficiency Increased by Very Fast Magic Angle Spinning, J. Am. Chem. Soc. 139 **(**2017**)** 10609–10612.

[14] A. Purea, C. Reiter, A. I. Dimitriadis, E. De Rijk, F. Aussenac, I. Sergeyev, M. Rosay, F. Engelke. Improved waveguide coupling for 1.3 mm MAS DNP probes at 263 GHz, J. Magn. Reson. 302 **(**2019**)** 43–49.

[15] P. Berruyer, S. Björgvinsdóttir, A. Bertarello, G. Stevanato, Y. Rao, G. Karthikeyan, G. Casano, O. Ouari, M. Lelli, C. Reiter, F. Engelke, L. Emsley. Dynamic Nuclear Polarization Enhancement of 200 at 21.15 T Enabled by 65 kHz Magic Angle Spinning, J. Phys. Chem. Lett. 11 **(**2020**)** 8386–8391.

[16] Z. Wang, M. P. Hanrahan, T. Kobayashi, F. A. Perras, Y. Chen, F. Engelke, C. Reiter, A. Purea, A. J. Rossini, M. Pruski. Combining fast magic angle spinning dynamic nuclear polarization with indirect detection to further enhance the sensitivity of solid-state NMR spectroscopy, Solid State Nucl. Magn. Reson. 109 **(**2020**)** 101685.

[17] A. A. Maudsley, R. R. Ernst. Indirect detection of magnetic resonance by heteronuclear two-dimensional spectroscopy, Chem. Phys. Lett. 50 **(**1977**)** 368–372.

[18] G. Bodenhausen, D. J. Ruben. Natural abundance nitrogen-15 NMR by enhanced heteronuclear spectroscopy, Chem. Phys. Lett. 69 **(**1980**)** 185–189.

[19] Y. Ishii, R. Tycko. Sensitivity Enhancement in Solid State ^{15}N NMR by Indirect Detection

with High-Speed Magic Angle Spinning, J. Magn. Reson. 142 **(**2000**)** 199–204.

[20] Y. Ishii, J. P. Yesinowski, R. Tycko. Sensitivity Enhancement in Solid-State 13 C NMR of Synthetic Polymers and Biopolymers by 1 H NMR Detection with High-Speed Magic Angle Spinning, J. Am. Chem. Soc. 123 **(**2001**)** 2921–2922.

[21] E. K. Paulson, C. R. Morcombe, V. Gaponenko, B. Dancheck, R. A. Byrd, K. W. Zilm. Sensitive high resolution inverse detection NMR spectroscopy of proteins in the solid state., J. Am. Chem. Soc. 125 **(**2003**)** 15831–15836.

[22] B. Reif, R. G. Griffin. ^{1}H detected ^{1}H,^{15}N correlation spectroscopy in rotating solids, J. Magn. Reson. 160 **(**2003**)** 78–83.

[23] T. Kobayashi, Y. Nishiyama, M. Pruski. Chapter 1. Heteronuclear Correlation Solid-state NMR Spectroscopy with Indirect Detection under Fast Magic-angle Spinning, in *New Developments in NMR* **(Royal Society of Chemistry, 2018).** 1–38. doi:10.1039/9781788010467-00001

[24] R. Tycko. Indirect detection in solid state NMR: An illustrious history and a bright future, J. Magn. Reson. 288 **(**2018**)** 122–123.

[25] J. Struppe, C. M. Quinn, S. Sarkar, A. M. Gronenborn, T. Polenova. Ultrafast ^{1}H MAS NMR Crystallography for Natural Abundance Pharmaceutical Compounds, Mol. Pharm. 17 **(**2020**)** 674–682.

[26] S. Asami, B. Reif. Proton-detected solid-state NMR spectroscopy at aliphatic sites: Application to crystalline systems, Acc. Chem. Res. 46 **(**2013**)** 2089–2097.

[27] L. B. Andreas, T. Le Marchand, K. Jaudzems, G. Pintacuda. High-resolution proton-

detected NMR of proteins at very fast MAS, J. Magn. Reson. 253 (2015) 36–49.

[28] K. Xue, R. Sarkar, C. Motz, S. Asami, D. C. R. Camargo, V. Decker, S. Wegner, Z. Tosner, B. Reif. Limits of Resolution and Sensitivity of Proton Detected MAS Solid-State NMR Experiments at 111 kHz in Deuterated and Protonated Proteins, Sci. Rep. 7 (2017) 1–7.

[29] C. Song, K. N. Hu, C. G. Joo, T. M. Swager, R. G. Griffin. TOTAPOL: A biradical polarizing agent for dynamic nuclear polarization experiments in aqueous media, J. Am. Chem. Soc. 128 (2006) 11385–11390.

[30] A. J. Rossini, A. Zagdoun, F. Hegner, M. Schwarzwälder, D. Gajan, C. Copéret, A. Lesage, L. Emsley. Dynamic Nuclear Polarization NMR Spectroscopy of Microcrystalline Solids, J. Am. Chem. Soc. 134 (2012) 16899–16908.

[31] C. Sauvée, M. Rosay, G. Casano, F. Aussenac, R. T. Weber, O. Ouari, P. Tordo. Highly efficient, water-soluble polarizing agents for dynamic nuclear polarization at high frequency, Angew. Chemie - Int. Ed. 52 (2013) 10858–10861.

[32] A. Zagdoun, G. Casano, O. Ouari, M. Schwarzwälder, A. J. Rossini, F. Aussenac, M. Yulikov, G. Jeschke, C. Copéret, A. Lesage, P. Tordo, L. Emsley. Large Molecular Weight Nitroxide Biradicals Providing Efficient Dynamic Nuclear Polarization at Temperatures up to 200 K, J. Am. Chem. Soc. 135 (2013) 12790–12797.

[33] A. P. Jagtap, M. A. Geiger, D. Stöppler, M. Orwick-Rydmark, H. Oschkinat, S. T. Sigurdsson. BcTol: A highly water-soluble biradical for efficient dynamic nuclear polarization of biomolecules, Chem. Commun. 52 (2016) 7020–7023.

[34] M. A. Geiger, A. P. Jagtap, M. Kaushik, H. Sun, D. Stöppler, S. T. Sigurdsson, B. Corzilius,

H. Oschkinat. Efficiency of Water-Soluble Nitroxide Biradicals for Dynamic Nuclear Polarization in Rotating Solids at 9.4 T: bcTol-M and cyolyl-TOTAPOL as New Polarizing Agents, Chem. – A Eur. J. 24 **(**2018**)** 13485–13494.

[35] F. Mentink-Vigier, I. Marin-Montesinos, A. P. Jagtap, T. Halbritter, J. van Tol, S. Hediger, D. Lee, S. T. Sigurdsson, G. De Paëpe. Computationally Assisted Design of Polarizing Agents for Dynamic Nuclear Polarization Enhanced NMR: The AsymPol Family, J. Am. Chem. Soc. 140 **(**2018**)** 11013–11019.

[36] A. Lund, G. Casano, G. Menzildjian, M. Kaushik, G. Stevanato, M. Yulikov, R. Jabbour, D. Wisser, M. Renom-Carrasco, C. Thieuleux, F. Bernada, H. Karoui, D. Siri, M. Rosay, I. V. Sergeyev, D. Gajan, M. Lelli, L. Emsley, O. Ouari, *et al.* TinyPols: A family of water-soluble binitroxides tailored for dynamic nuclear polarization enhanced NMR spectroscopy at 18.8 and 21.1 T, Chem. Sci. 11 **(**2020**)** 2810–2818.

[37] G. Mathies, M. A. Caporini, V. K. Michaelis, Y. Liu, K.-N. Hu, D. Mance, J. L. Zweier, M. Rosay, M. Baldus, R. G. Griffin. Efficient Dynamic Nuclear Polarization at 800 MHz/527 GHz with Trityl-Nitroxide Biradicals, Angew. Chemie Int. Ed. 54 **(**2015**)** 11770–11774.

[38] F. Mentink-Vigier, G. Mathies, Y. Liu, A.-L. A.-L. L. Barra, M. A. M. A. Caporini, D. Lee, S. Hediger, R. Griffin, G. De Paëpe, R. G. Griffin, G. De Paëpe. Efficient cross-effect dynamic nuclear polarization without depolarization in high-resolution MAS NMR, Chem. Sci. 8 **(**2017**)** 8150–8163.

[39] W. Zhai, A. Lucini Paioni, X. Cai, S. Narasimhan, J. Medeiros-Silva, W. Zhang, A. Rockenbauer, M. Weingarth, Y. Song, M. Baldus, Y. Liu. Postmodification via Thiol-Click Chemistry Yields Hydrophilic Trityl-Nitroxide Biradicals for Biomolecular High-Field

Dynamic Nuclear Polarization, J. Phys. Chem. B 124 (2020) 9047–9060.

[40] D. Wisser, G. Karthikeyan, A. Lund, G. Casano, H. Karoui, M. Yulikov, G. Menzildjian, A. C. Pinon, A. Purea, F. Engelke, S. R. Chaudhari, D. Kubicki, A. J. Rossini, I. B. Moroz, D. Gajan, C. Copéret, G. Jeschke, M. Lelli, L. Emsley, *et al.* BDPA-Nitroxide Biradicals Tailored for Efficient Dynamic Nuclear Polarization Enhanced Solid-State NMR at Magnetic Fields up to 21.1 T, J. Am. Chem. Soc. 140 (2018) 13340–13349.

[41] F. Mentink-Vigier, U. Akbey, Y. Hovav, S. Vega, H. Oschkinat, A. Feintuch. Fast passage dynamic nuclear polarization on rotating solids, J. Magn. Reson. 224 (2012) 13–21.

[42] K. R. Thurber, R. Tycko. Perturbation of nuclear spin polarizations in solid state NMR of nitroxide-doped samples by magic-angle spinning without microwaves, J. Chem. Phys. 140 (2014) 184201.

[43] F. Mentink-Vigier, S. Paul, D. Lee, A. Feintuch, S. Hediger, S. Vega, G. De Paëpe. Nuclear depolarization and absolute sensitivity in magic-angle spinning cross effect dynamic nuclear polarization, Phys. Chem. Chem. Phys. 17 (2015) 21824–21836.

[44] F. Mentink-Vigier, Ü. Akbey, H. Oschkinat, S. Vega, A. Feintuch. Theoretical aspects of Magic Angle Spinning - Dynamic Nuclear Polarization, J. Magn. Reson. 258 (2015) 102–120.

[45] F. Mentink-Vigier, S. Vega, G. De Paëpe. Fast and accurate MAS–DNP simulations of large spin ensembles, Phys. Chem. Chem. Phys. 19 (2017) 3506–3522.

[46] R. Harrabi, T. Halbritter, F. Aussenac, O. Dakhlaoui, J. van Tol, K. K. Damodaran, D. Lee, S. Paul, S. Hediger, F. Mentink-Vigier, S. T. Sigurdsson, G. De Paëpe. Highly Efficient

Polarizing Agents for MAS-DNP of Proton-Dense Molecular Solids, Angew. Chemie Int. Ed. 61 **(**2022**)** e202114103.

[47] I. Matlahov, P. C. A. van der Wel. Conformational studies of pathogenic expanded polyglutamine protein deposits from Huntington's disease, Exp. Biol. Med. 244 **(**2019**)** 1584–1595.

[48] G. Teymoori, B. Pahari, B. Stevensson, M. Edén. Low-power broadband homonuclear dipolar recoupling without decoupling: Double-quantum ^{13}C NMR correlations at very fast magic-angle spinning, Chem. Phys. Lett. 547 **(**2012**)** 103–109.

[49] G. Teymoori, B. Pahari, M. Edén. Low-power broadband homonuclear dipolar recoupling in MAS NMR by two-fold symmetry pulse schemes for magnetization transfers and double-quantum excitation, J. Magn. Reson. 261 **(**2015**)** 205–220.

[50] T. Biedenbänder, V. Aladin, S. Saeidpour, B. Corzilius. Dynamic Nuclear Polarization for Sensitivity Enhancement in Biomolecular Solid-State NMR, Chem. Rev. 122 **(**2022**)** 9738–9794.

[51] W. Y. Chow, G. De Paëpe, S. Hediger. Biomolecular and Biological Applications of Solid-State NMR with Dynamic Nuclear Polarization Enhancement, Chem. Rev. 122 **(**2022**)** 9795–9847.

[52] A. N. Smith, K. Märker, T. Piretra, J. C. Boatz, I. Matlahov, R. Kodali, S. Hediger, P. C. A. van der Wel, G. De Paëpe. Structural Fingerprinting of Protein Aggregates by Dynamic Nuclear Polarization-Enhanced Solid-State NMR at Natural Isotopic Abundance, J. Am. Chem. Soc. 140 **(**2018**)** 14576–14580.

[53] L. Zhao, A. C. Pinon, L. Emsley, A. J. Rossini. DNP-enhanced solid-state NMR spectroscopy of active pharmaceutical ingredients, Magn. Reson. Chem. 56 **(**2018**)** 583–609.

[54] A. N. Smith, K. Märker, S. Hediger, G. De Paëpe. Natural Isotopic Abundance ^{13}C and ^{15}N Multidimensional Solid-State NMR Enabled by Dynamic Nuclear Polarization, J. Phys. Chem. Lett. 10 **(**2019**)** 4652–4662.

[55] A. Kirui, Z. Ling, X. Kang, M. C. Dickwella Widanage, F. Mentink-Vigier, A. D. French, T. Wang. Atomic resolution of cotton cellulose structure enabled by dynamic nuclear polarization solid-state NMR, Cellulose 26 **(**2019**)** 329–339.

[56] W. Zhao, A. Kirui, F. Deligey, F. Mentink-Vigier, Y. Zhou, B. Zhang, T. Wang. Solid-state NMR of unlabeled plant cell walls: high-resolution structural analysis without isotopic enrichment, Biotechnol. Biofuels 14 **(**2021**)** 14.

[57] S. Wi, N. Dwivedi, R. Dubey, F. Mentink-Vigier, N. Sinha. Dynamic nuclear polarization-enhanced, double-quantum filtered ^{13}C-^{13}C dipolar correlation spectroscopy of natural ^{13}C abundant bone-tissue biomaterial, J. Magn. Reson. 335 **(**2022**)** 107144.

[58] H. Takahashi, D. Lee, L. Dubois, M. Bardet, S. Hediger, G. De Paëpe. Rapid Natural-Abundance 2D ^{13}C-^{13}C Correlation Spectroscopy Using Dynamic Nuclear Polarization Enhanced Solid-State NMR and Matrix-Free Sample Preparation, Angew. Chemie Int. Ed. 51 **(**2012**)** 11766–11769.

[59] H. Takahashi, S. Hediger, G. De Paëpe. Matrix-free dynamic nuclear polarization enables solid-state NMR ^{13}C–^{13}C correlation spectroscopy of proteins at natural isotopic abundance, Chem. Commun. 49 **(**2013**)** 9479–9481.

[60] A. J. Rossini, C. M. Widdifield, A. Zagdoun, M. Lelli, M. Schwarzwälder, C. Copéret, A. Lesage, L. Emsley. Dynamic nuclear polarization enhanced NMR spectroscopy for pharmaceutical formulations, J. Am. Chem. Soc. 136 **(**2014**)** 2324–2334.

[61] K. Märker, M. Pingret, J. M. Mouesca, D. Gasparutto, S. Hediger, G. De Paëpe. A New Tool for NMR Crystallography: Complete $^{13}C/^{15}N$ Assignment of Organic Molecules at Natural Isotopic Abundance Using DNP-Enhanced Solid-State NMR, J. Am. Chem. Soc. 137 **(**2015**)** 13796–13799.

[62] G. Mollica, M. Dekhil, F. Ziarelli, P. Thureau, S. Viel. Quantitative Structural Constraints for Organic Powders at Natural Isotopic Abundance Using Dynamic Nuclear Polarization Solid-State NMR Spectroscopy, Angew. Chemie Int. Ed. 54 **(**2015**)** 6028–6031.

[63] A. C. Pinon, A. J. Rossini, C. M. Widdifield, D. Gajan, L. Emsley. Polymorphs of Theophylline Characterized by DNP Enhanced Solid-State NMR, Mol. Pharm. 12 **(**2015**)** 4146–4153.

[64] K. Märker, S. Paul, C. Fernández-de-Alba, D. Lee, J.-M. Mouesca, S. Hediger, G. De Paëpe. Welcoming natural isotopic abundance in solid-state NMR: probing π-stacking and supramolecular structure of organic nanoassemblies using DNP, Chem. Sci. 8 **(**2017**)** 974–987.

[65] T. Kobayashi, I. I. Slowing, M. Pruski. Measuring Long-Range 13 C– 13 C Correlations on a Surface under Natural Abundance Using Dynamic Nuclear Polarization-Enhanced Solid-State Nuclear Magnetic Resonance, J. Phys. Chem. C 121 **(**2017**)** 24687–24691.

[66] A. Lesage, L. Emsley. Through-Bond Heteronuclear Single-Quantum Correlation Spectroscopy in Solid-State NMR, and Comparison to Other Through-Bond and Through-

Space Experiments, J. Magn. Reson. 148 (2001) 449–454.

[67] G. De Paëpe. Dipolar Recoupling in Magic Angle Spinning Solid-State Nuclear Magnetic Resonance, Annu. Rev. Phys. Chem. 63 (2012) 661–684.

[68] P. C. A. van der Wel, K.-N. Hu, J. Lewandowski, R. G. Griffin. Dynamic Nuclear Polarization of Amyloidogenic Peptide Nanocrystals: GNNQQNY, a Core Segment of the Yeast Prion Protein Sup35p, J. Am. Chem. Soc. 128 (2006) 10840–10846.

[69] A. Hofstetter, M. Balodis, F. M. Paruzzo, C. M. Widdifield, G. Stevanato, A. C. Pinon, P. J. Bygrave, G. M. Day, L. Emsley. Rapid Structure Determination of Molecular Solids Using Chemical Shifts Directed by Unambiguous Prior Constraints, J. Am. Chem. Soc. 141 (2019) 16624–16634.

[70] R. Tycko. Solid-State NMR Studies of Amyloid Fibril Structure, Annu. Rev. Phys. Chem. 62 (2011) 279–299.

[71] W. Qiang, W.-M. Yau, J.-X. Lu, J. Collinge, R. Tycko. Structural variation in amyloid-β fibrils from Alzheimer's disease clinical subtypes, Nature 541 (2017) 217–221.

[72] K. K. Frederick, V. K. Michaelis, B. Corzilius, T. C. Ong, A. C. Jacavone, R. G. Griffin, S. Lindquist. Sensitivity-Enhanced NMR Reveals Alterations in Protein Structure by Cellular Milieus, Cell 163 (2015) 620–628.